Magnetic phase diagram of a molecule-based ferrimagnet: Weak ferromagnetism and multiple dimensionality crossovers

C. M. Wynn and M. A. Gîrţu
Department of Physics, The Ohio State University, Columbus, Ohio 43210-1106

Joel S. Miller
Department of Chemistry, University of Utah, Salt Lake City, Utah 84112

A. J. Epstein
Department of Physics and Department of Chemistry, The Ohio State University, Columbus, Ohio, 43210-1106

(Received 16 June 1997)

A detailed study of the magnetic behavior of the molecule-based magnet, [MnOEP][HCBD], (OEP=*meso*-octaethylporphyrinato, HCBD=hexacyanobutadiene) from 1.7 to 20 K was performed. The earlier reported magnetic transition at 19.6 K, ascribed to a crossover from a one-dimensional Heisenberg-like ferrimagnet to a two-dimensional Ising-like antiferromagnet, is further probed via ac-dc magnetic studies consisting of dc magnetization as a function of field at various temperatures, and magnetization as a function of temperature with both field cooling and zero-field cooling. In addition, the ac susceptibility was measured as a function of temperature and applied dc field. The appearance of a nonzero out-of-phase component of the ac susceptibility in zero dc field at 8 K accompanied by a shoulder in the in-phase component indicates the presence of a magnetic transition near that temperature. Irreversibilities and a spontaneous moment observed below 4.2 K indicate an additional lower temperature transition. The ac and dc data allow a determination of the temperature-field phase boundaries around these transitions. Evidence of a tricritical point at 2 kOe and 19.6 K and a multicritical point at 9.5 kOe and 8 K is presented. The nature of the ordered states, along with the possible mechanisms responsible for the transitions, including dipole-dipole interactions, are analyzed. [S0163-1829(97)02446-6]

I. INTRODUCTION

The Mn(III)-porphyrin/cyanocarbon donor-acceptor family of electron transfer salts has been of increasing interest in recent years.[1–4] This family of quasi-one-dimensional (1D) molecule-based magnets are alternating $S=2$, $s=1/2$ ferrimagnetic linear chains with relatively large intrachain interactions ($|J|>50$ K).[5] Via synthetic chemistry it has been possible to subtly affect parameters such as intra- and interchain exchange and local spin anisotropy thus shedding light on the fundamental mechanisms governing the magnetic interactions, the effects of disorder, and also the effects of spin and lattice dimensionalities and dimensionality crossovers.

[Mn(III)OEP][HCBD], (OEP=*meso*-octaethylporphyrinato and HCBD=hexacyanobutadiene) is important because it is one of the few members of the family showing no evidence of structural disorder and/or glassiness.[6] As such it is an important reference to which other more complicated members of the family may be compared. The compound consists of ($S=2$) $[Mn(III)OEP]^+$ donor cations trans-μ_2-bonded to ($s=1/2$) $[HCBD]^-$ acceptor anions in a linear chain structure.[1] Earlier studies[7] revealed the presence of a magnetic transition at 19.6 K attributed to a transition from a one-dimensional Heisenberg-like ferrimagnet to a two-dimensional Ising-like state due to weak antiferromagnetic (AFM) exchange between chains forming a plane.

In this paper, we present a detailed study of the magnetic states of this compound at and below its transition at 19.6 K. Evidence is presented for magnetic transitions at 8 and 4.2 K to weak ferromagnetic states. Based on ac and dc magnetic studies, a detailed phase diagram is constructed. Mechanisms responsible for the ordered states are discussed in light of recent evidence[8] that dipole-dipole interactions are responsible for the low-temperature ordering and resultant weak ferromagnetism in this compound and other members of the family. The outline of this paper is as follows. In Sec. II, we discuss the experimental apparatus and techniques, in Sec. III we report the results of ac (in zero and finite dc fields) and dc susceptibility and magnetization studies. Section IV consists of a discussion of these data and presentation of the resulting phase diagram. Section V summarizes our conclusions.

II. EXPERIMENT

Magnetization M data were collected using a Quantum Design Model MPMS-5 superconducting quantum interference device magnetometer with a continuous-flow cryostat and a 5.5 T superconducting solenoid. Susceptibility data were recorded on a Lake Shore Model 7225 ac susceptometer with an exchange cryostat and 5.0 T superconducting solenoid. Phase sensitive measurements were made using a lock-in amplifier. Previous studies[7] revealed no frequency dependence of the ac susceptibility above the lowest attainable temperature of 1.7 K and within the frequency range of 5–10 000 Hz. All measurements were thus recorded at 1 kHz. A dc bias field H of 0–2 T was used in addition to the ac field, which was kept at a constant 1 Oe. Calibration of

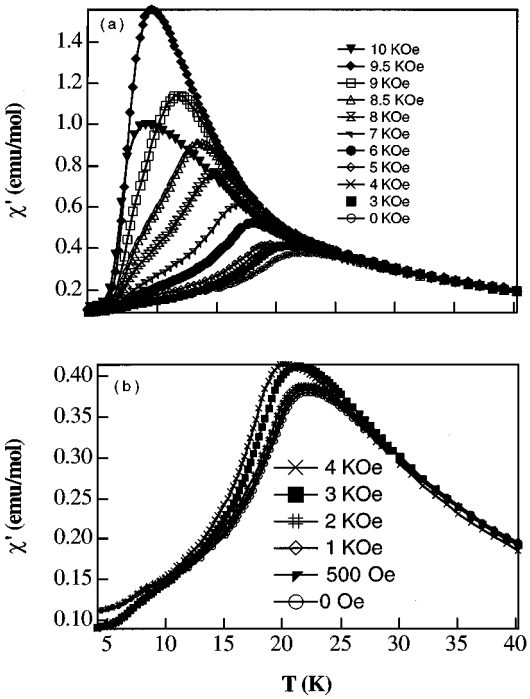

FIG. 1. (a) In-phase ac susceptibility, χ' as a function of temperature, T as measured in various dc fields (legend), (b) closeup of low-field data.

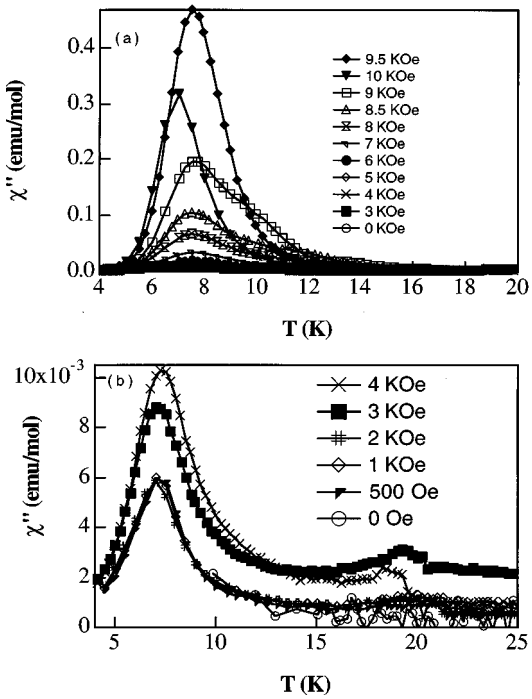

FIG. 2. (a) Out-of-phase ac susceptibility, χ'' as a function of temperature, T as measured in various dc fields (legend), (b) closeup of low-field data.

the absolute magnitude of the susceptibility along with determination of the proper phases of the instrument were made using a $HgCo(SCN)_4$ paramagnetic material. The dc susceptibility, χ_{dc}, was taken as M/H. All magnetic data were taken on powder samples that had been sealed under argon in quartz EPR tubes to avoid contamination with air. The largest uncertainties in the magnetic data ($\pm 2\%$) arose from the error in measuring the sample mass. Corrections for diamagnetism were made using $\chi_{dia} = -4.83 \times 10^{-4}$ emu/mol as obtained from Pascal's constants.[9] The diamagnetism of the quartz sample holders was separately measured and subtracted from the data.

III. RESULTS

A. ac susceptibility

Both the in-phase, $\chi'_H(T)$, and out-of-phase, $\chi''_H(T)$, components of the complex ac susceptibility were measured as a function of temperature from 1.7 to 40 K, in constant dc fields ranging from 0 to 10 kOe (Figs. 1 and 2). In zero dc field, as previously reported,[7] a maximum in $\chi'_0(T)$ occurs at 22.5 K with a value of 0.42 emu/mol. A maximum in $\chi''_0(T)$ occurs at 7.5 K with a value of 0.006 emu/mol, along with an accompanying shoulder in $\chi'_0(T)$. Direct current field dependence of the both $\chi'_H(T)$ and $\chi''_H(T)$ occurs for $H > 2$ kOe. As the dc field is increased from 2 to 9.5 kOe, the temperature of the peak in $\chi'_H(T)$ decreases, and the magnitude of the peak increases. At 9.5 kOe, the magnitude of $\chi'_H(T)$ is maximized, being 1.56 emu/mol at its peak temperature of 9.4 K. At 10 kOe, the magnitude of the peak in $\chi'_H(T)$ decreases relative to its value at 9.5 kOe, falling to a value of 1.00 emu/mol at its peak temperature of 9.0 K. The 7.5 K shoulder in $\chi'_H(T)$ remains at a relatively constant temperature (within 0.2 K) for $H < 9.5$ kOe, above which it becomes difficult to distinguish the shoulder from the main peak. The magnitude of the 7.5 K peak in $\chi''_H(T)$ increases as H is increased from 2 to 9.5 kOe, however, the peak temperature remains constant. The maximum value (0.52 emu/mol) of the 7.5 K peak in $\chi''_H(T)$ occurs at 9.5 kOe. At 10 kOe, the magnitude of the peak in $\chi''_H(T)$ decreases to 0.34 emu/mol, and the temperature of the peak decreases to 7 K. A shoulder in $\chi_H{}'(T)$ is evident for $H > 2$ kOe. It occurs at 19 K [near the main peak in $\chi_H{}'(T)$] for $H = 3$ kOe, and decreases in temperature with increasing field, eventually merging with the lower temperature peak in $\chi_H{}'(T)$.

Isothermal measurements of both $\chi'_T(H)$ and $\chi''_T(H)$ for $0 < H < 40$ kOe were made at temperatures from 4.2 to 23 K (Figs. 3 and 4). At 19 K (below the previously determined transition temperature of 19.6 K), $\chi'_T(H)$ shows a maximum (0.52 emu/mol) at 9.1 kOe; the field of this maximum increases as the temperature is decreased, reaching a value of 24.0 kOe at 4.2 K. The magnitude of the maximum in $\chi'_T(H)$ increases with decreasing temperature until ~9 K, after which it decreases in magnitude. $\chi''_T(H)$ shows no signal above ~15 K, at which point it displays a narrow peak, ~2 kOe wide, (maximum value=0.005 emu/mol) centered at 8 kOe. As the temperature is lowered below 15 K, the peak broadens, and the field of the maximum increases, reaching a value of 20.4 kOe at 4.2 K. The magnitude of the peak in $\chi''_T(H)$ increases with decreasing temperature from 15 to ~7 K, below which it decreases in magnitude.

B. dc magnetization and dc susceptibility

Previous isothermal studies[7] of M as a function of H for 5 K $< T <$ 25 K revealed a rapid increase of $M(H)$ near 10 kOe

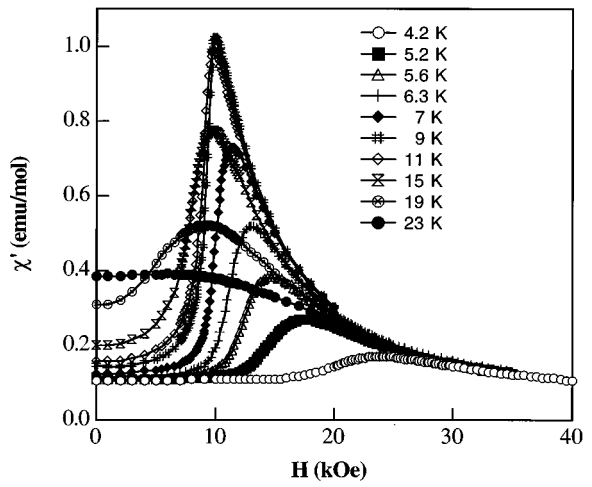

FIG. 3. Isothermal in-phase ac susceptibility, χ' as a function of field, H at various temperatures (legend).

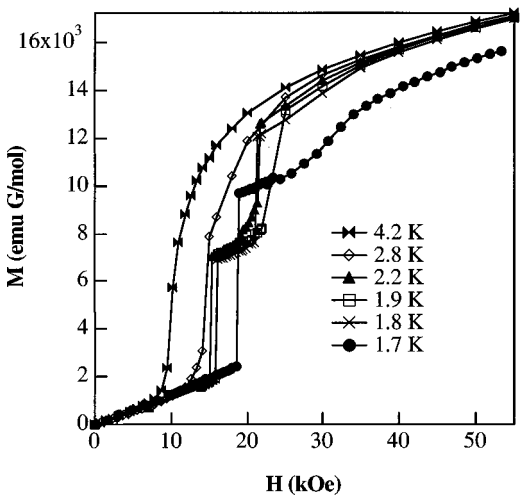

FIG. 5. Isothermal magnetization, M as a function of field, H at various temperatures (legend).

at temperatures below 19.6 K, indicative of a metamagnetic transition. Figure 5 displays isothermal $M(H)$ curves for $T < 5$ K, revealing behavior resembling metamagnetism in which the magnetization is linear with field below a certain field and subsequently increases rapidly before approaching the saturation value of 16 800 emu G/mol expected for ferrimagnetically aligned spins. At 4.2 K and below, the initial linear part of the curve extends beyond 10 kOe (in contrast to the behavior above 5 K for which the linear region never extends beyond 10 kOe), reaching ~20 kOe at 1.7 K. Between 1.8 and 2.2 K the magnetization shows steplike behavior in which $M(H)$ increases abruptly near 15 kOe to ~7 000 emuG/mol, then increases again near 22 kOe to ~12 000 emuG/mol, after which it approaches saturation, indicating a transition additional to the single metamagnetic transition observed at higher temperatures. At 1.7 K, the lowest attainable temperature, the magnetization increases linearly with field until it abruptly (data were collected in 50 Oe increments near the transition yet no points intermediate to the low and high magnetization states were measured) jumps to ~10 000 emuG/mol at 19 kOe, after which it undergoes an inflection point near 25 kOe and 12 000 emuG/mol before approaching saturation. The maximum observed ($H = 55$ kOe) value of the isothermal magnetization at 1.7 K is reduced relative to the higher temperature curves displayed in Fig. 5, indicating the possibility of an additional transition for $H > 55$ kOe.

Three different types of isothermal hysteresis curves were observed from 1.7 to 40 K. Above 8 K, no irreversibilities were observed. From 4.2 to 8 K, the curves show irreversibility, but zero coercive field. A curve typical of this region, at 7 K, is displayed in Fig. 6. The curve shows irreversibility from 0 to 10 kOe, however, it is constricted at the origin with zero measurable coercive field. Below 4.2 K, the curves are

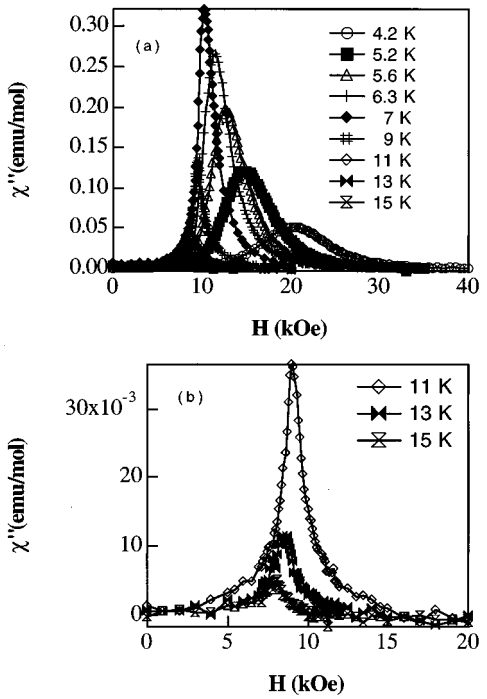

FIG. 4. (a) Isothermal out-of-phase ac susceptibility, χ'' as a function of field, H at various temperatures (legend), (b) closeup of higher temperature data.

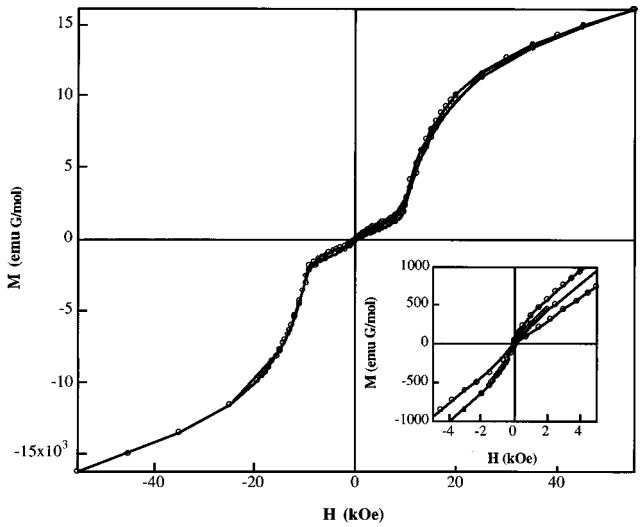

FIG. 6. Full hysteresis loop showing magnetization, M as a function of field, H at 7 K. Inset shows a closeup of the low-field data.

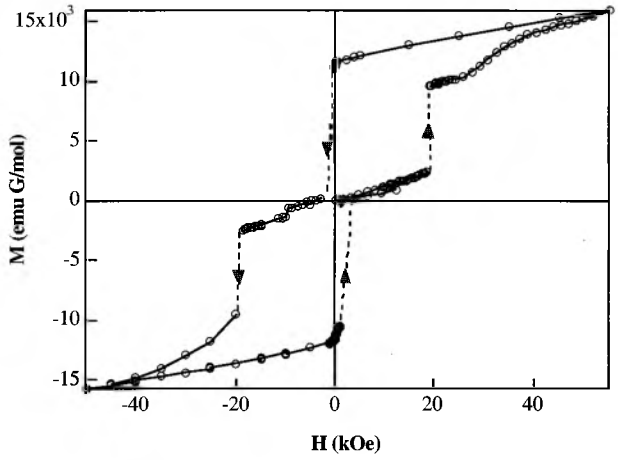

FIG. 7. Full hysteresis loop showing magnetization, M as a function of field, H at 1.7 K.

constricted at the origin, but with nonzero coercive fields. Figure 7 displays a hysteresis loop with a coercive field of ~4 kOe at 1.7 K.

The field-cooled (FC) and zero-field cooled (ZFC) dc susceptibilities were measured in various applied fields (Fig. 8), and showed a bifurcation near 4 K that was independent of the measuring field. The remanent moment was measured by cooling the compound in a field of 40 Oe to 1.7 K, zeroing the field at 1.7 K, and recording the remanent magnetization as a function of temperature while warming. The remanence vanishes above 4.2 K (Fig. 9).

IV. DISCUSSION

A. Transitions in zero field

For $H=0$, previously reported[7] magnetic studies indicate a transition at $T=19.6$ K from a 1D Heisenberg-like ferrimagnet to a system of two-dimensionally (2D) antiferromagnetically coupled Ising-like chains, represented by the following Hamiltonian:

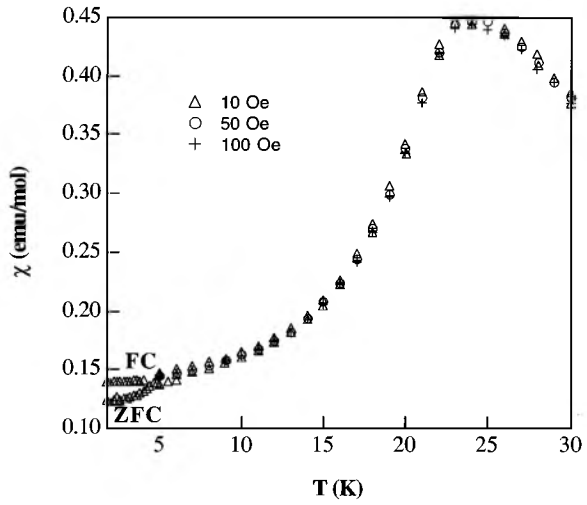

FIG. 8. Field-cooled (FC) and zero-field-cooled (ZFC) dc susceptibilities as a function of temperature, T as measured in various fields (legend).

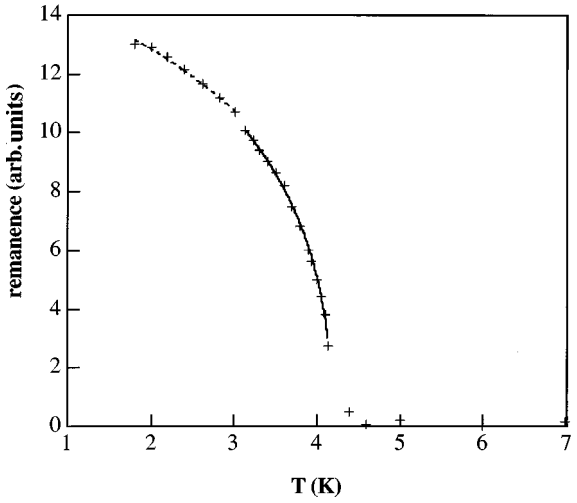

FIG. 9. Remanent magnetization as a function of temperature, T. Data were recorded by cooling in 40 Oe to 1.7 K, zeroing the field and recording remanence while warming. Solid line is a fit (3.4 K$\leq T\leq$4.2 K) to a power law in reduced temperature. Dashed line (1.8 K $\leq T\leq$3.2 K) is a fit to the D-M predictions for a canted antiferromagnet below its ordering temperature.

$$\mathcal{H}=-2J_{\text{intra}}\sum_{i,j}\mathbf{S}_{i,j}\cdot\mathbf{S}_{i,j+1}-2J_{\text{inter}}\sum_{i,j}\mathbf{S}_{i,j}\cdot\mathbf{S}_{i+1,j}+\sum_{i}DS_{z,i}^{2}, \tag{1}$$

where J_{intra} and J_{inter} represent the intra- and interchain exchange strengths respectively, and $DS_{z,i}^2$ is the contribution due to single-ion anisotropy. The previous work[7] yielded values of $J_{\text{intra}}=-172$ K, $J_{\text{inter}}=-0.4$ K, and $D\sim-3$ K (negative D corresponds to an Ising-like system). In this section, we analyze the zero-field data below 19.6 K, concluding that transitions additional to those expected for the 2D AFM state (see discussion below) occur, indicative of further dimensionality crossovers and additional terms in the Hamiltonian.

In theory, a magnetic transition is marked by a diverging magnetic specific heat. For an AFM, the susceptibility is related to the magnetic specific heat c, through theoretical relationships derived by Fisher[10] relating it to the absolute value of the magnetic energy, $\partial(\chi_{\text{H}}'T)/\partial T\sim c$. Figure 10 displays the experimental $\partial(\chi_{\text{H}}'T)/\partial T$ as a function of temperature as measured in zero and applied fields. Two peaks are observed in all curves, each slightly below the corresponding peaks in $\chi_H'(T)$. These data indicate two transitions.

The peak at 19.6 K in zero field represents the previously discussed 2D AFM transition, while the smaller peak at 8 K supports an additional phase transition. Below 8 K, a nonzero $\chi_H''(T)$ is observed along with hysteresis in the $M_{\text{dc}}(H)$ curves and a difference between the ac and dc data. These data are indicative of a spontaneous moment[11] not expected in AFM systems, suggesting the system is no longer behaving as a simple AFM and has undergone another phase transition. This 8 K transition is consistent with the observation of a tricritical point at 19.6 K and 2 kOe that indicates FM interchain interactions additional to the AFM interchain interactions (see next section). While some of the data suggests

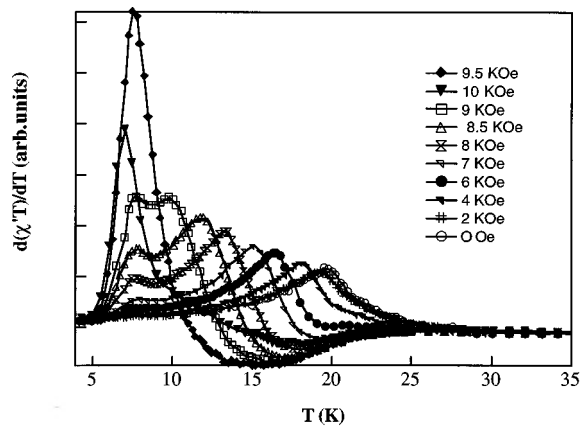

FIG. 10. Derivative of $\chi' T$ with respect to T as a function of temperature, T as measured in various fields (legend).

ferromagnetic character near 8 K, no evidence of a diverging χ (indicative of a pure FM transition) including successful FM scaling analyses collapsing $M(H,T)$ data to a universal curve, is found. These data, in addition to the constricted hysteresis curves similar to those observed in weak ferromagnets,[12,13] suggest a weak ferromagnetic (or canted AFM) state below 8 K. The following addition to the Hamiltonian is proposed:

$$\mathbf{d}\cdot\mathbf{S_i}\times\mathbf{S_j}, \tag{2}$$

where $\mathbf{d}$ is the Dzialoshinski-Moriya tensor. The bulk response of the powdered material contains components both parallel and perpendicular to the weak ferromagnetic moment.

The dimensionality of the 8 K transition is now discussed. While the irreversibilities in the data (χ'' of Fig. 2) indicate a spontaneous moment, bulk dc measurements (Fig. 9) show no remanence. The absence of a measurable remanence suggests a 2D configuration in which the chains are coupled into sheets with spins on neighbor chains within the sheets canted relative to one another. Theoretically, such a configuration would give rise to a net moment within a sheet, which would give rise to losses and a nonzero χ'', but zero bulk dc moment as the sheets are not strongly correlated with one another and the sum of their individual moments averages to zero in the bulk. We also note that a transition to a ''soft'' 3D magnet, which would result in reversible magnetization giving rise to zero remanence, is not consistent with the data showing irreversibilities between 0 and 10 kOe (Fig. 6). The description as a 2D system is also consistent with the observation of a 3D transition at 4.2 K (see below). Thus we take the χ'' at 8 K and dc hysteresis loops with no remanence as evidence for a transition from a 2D Ising-like AFM to a 2D weak ferromagnet at 8 K.

Another transition is evident at 4.2 K. Below 4.2 K, a spontaneous moment is directly observed (Fig. 9) in addition to nonzero coercive fields, and differences in the FC and ZFC susceptibilities (Fig. 8). In theory, a spontaneous moment is related to the FM order parameter and should vanish continuously at the critical temperature according to[14]

$$M\sim t^{\beta} \tag{3}$$

where t is the reduced temperature $(T_c-T)/T_c$, and β is the critical exponent determined by dimensionality. A best fit to this power-law behavior for 3.4 K $\leqslant$ T $\leqslant$ 4.2 K, Fig. 9, yields a critical temperature of T_c=4.2 K, with critical exponent β=0.31±0.02. For a three-dimensional transition, β is expected to take values of 0.31 (3D Ising) to 0.37 (3D Heisenberg).[14,15] The value of β=0.31, along with the independence of the FC/ZFC bifurcation point on measuring field indicate a transition at 4.2 K to a 3D Ising-like system with no disorder suggesting either of the following additions to the Hamiltonian:

$$J_{3d}\mathbf{S_i}\cdot\mathbf{S_j} \tag{4}$$

or

$$\frac{1}{r^3}[\mathbf{S_i}\cdot\mathbf{S_j}-3(\mathbf{S_i}\cdot\mathbf{r})(\mathbf{S_j}\cdot\mathbf{r})/r^2], \tag{5}$$

where r is the distance between spin centers and J_{3d} is the exchange interaction between spins in neighboring planes. The dipole interaction energy between planes is estimated to be ~0.02 K (see Sec. IV C), much less than the intralayer interactions. The lack of magnetic disorder is unusual in this family of metalloporphyrins.[16]

Similar to the behavior near 8 K, a traditional FM scaling analysis was unsuccessful at 4.2 K. The lack of scaling, in addition to the constricted hysteresis curves below 4.2 K indicative of weak ferromagnetism, suggests a canted 3D state in which the sheets of chains with canted spins that formed at 8 K are coupled three dimensionally resulting in a bulk weak ferromagnetic moment. The experimental low-temperature $\chi'_H(T)$ Ref. 8 approaches a nonzero constant below ~ 4 K in accord with the Dzialoshinski and Moriya predictions for canted systems.[17] The spontaneous moment of a canted system in its ordered state, and well below the critical region near T_c, is predicted using spin-wave theory, based on a two-sublattice model, to behave as

$$M\sim[1-\eta(T/T_c)^2], \tag{6}$$

with η typically near 0.48.[18] A value of η=0.50±0.02 was obtained from a fit of the low-temperature (1.8 K$\leqslant T\leqslant$3.2 K) magnetization to this function while fixing T_c at 4.2 K (Fig. 9). Thus, the remanence and FC/ZFC data indicate a transition from 2D weak ferromagnet to 3D weak ferromagnet at 4.2 K.

B. Transitions in applied fields

In this section, we use our combined ac and dc data to map out the H-T phase boundaries below 19.6 K. Analysis of the data indicate the presence of a mixed phase and both tricritical and multicritical points.

The behavior of an anisotropic AFM below its Néel temperature, T_N, has been well investigated.[12] Below T_N, such antiferromagnets undergo two first-order phase transitions as the external field is isothermally increased from zero, the first from an AFM to a mixed phase (consisting of a mixture of both ferro- and antiferromagnetic domains) and the second from the mixed phase to a paramagnetic phase. If, in addition to the AFM interactions, there exist ferromagnetic interactions, then there will be a temperature below T_N

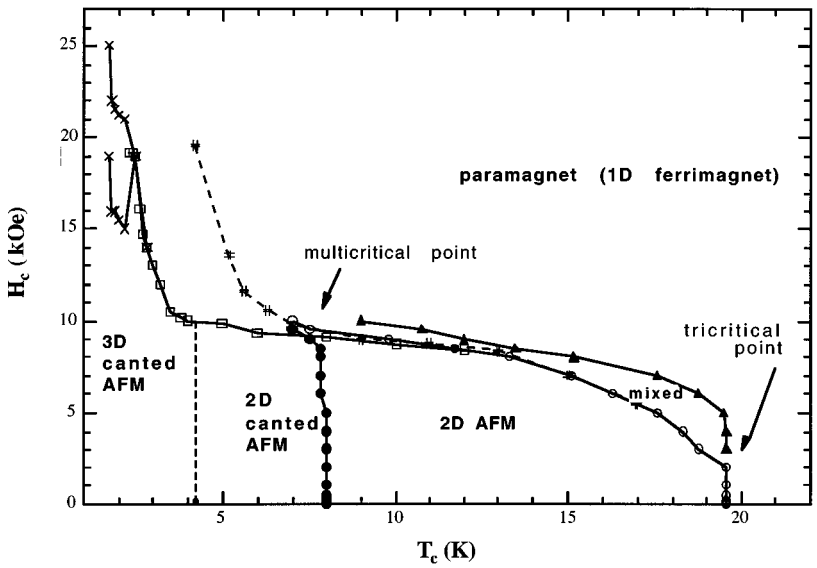

FIG. 11. Proposed phase diagram from ac and dc susceptibility and magnetization measurements. Based on peaks in $\partial(\chi'_H T)/\partial T$ (open, closed circles), disappearance of $\chi''_H(T)$ (filled triangles), maximum slope in $\chi'_T(H)$ (#), maximum slope in $dM_{dc}/dH_T(H)$ (open squares), low-temperature steps in $M(H)$ (crosses). Lines are guides to the eye.

(known as the tricritical point), above which only one transition occurs as an external field is isothermally applied, a second-order transition from AFM to paramagnet.[19] Below the tricritical temperature, both the AFM-mixed and mixed-paramagnetic transitions occur.

We utilize our $\chi_H(T)$ and $\chi_T(H)$ data to map the H-T phase boundary. In Fig. 10, we observe the temperature of the larger peak in $\partial(\chi'_H T)/\partial T$ decreasing monotonically as the measuring field is increased, similar to the expected behavior of the Neél temperature. As we did for $H=0$, we use the peak in $\partial(\chi'_H T)/\partial T$ (see Fig. 10) to mark the AFM-mixed transition temperature at each field (Fig. 11). This is consistent with other determinations of this H-T boundary, as will be discussed later in this section.

Our determination of the AFM-mixed phase boundary via $\chi'_T(H)$ is based on the following. In theory, when an external magnetic field of order of the AFM exchange strength is applied to an Ising-like AFM in its ordered state, the sublattice whose magnetization is opposite the field aligns with the field, giving rise to a sudden increase in the magnetization. The presence of a demagnetizing factor N, which reduces the internal field H_i, relative to the external field according to $H_i = H - NM$, suppresses the increase in M and forces the creation of the mixed state. While in the mixed state, the internal field remains constant despite an increase in the external field, and the susceptibility is limited by $1/N$. We thus use the point of maximum slope[20] in our $\chi'_T(H)$ data (see Fig. 3), and also $dM_{dc}/dH_T(H)$, to mark the AFM- mixed transition. The previously reported[7] dc curves are used to examine $dM_{dc}/dH_T(H)$ above 4.2 K. These results are displayed in Fig. 11. Both the ac and dc determinations coincide with the determination made using $\partial(\chi'_H T)/\partial T$; however, below 8 K at which a second transition is evident (see discussion below) the maximum slope in $dM_{dc}/dH_T(H)$ occurs at a lower field than $\chi'_T(H)$, i.e., the ac and dc data no longer coincide.

The mixed phase of a metamagnet consists of a mixture of both ferro- and antiferromagnetic domains. The transition from the mixed to the paramagnetic state should be marked by the disappearance of these domains, thus we use the point at which χ'' disappears to mark this boundary. Points using this criterion at the higher temperature shoulder of $\chi''_H(T)$ (see Fig. 4) are included in Fig. 11.

Near 19.6 K, $\chi''_H(T)$ vanishes for $H \lesssim 2$ kOe . The field dependence of both $\chi'_H(T)$ and $\chi''_H(T)$ occurs only for $H \gtrsim 2$ kOe . Interestingly, the curves of Fig. 11 indicate a tricritical point at 19.6 K and 2 kOe, from which three phases (paramagnetic, mixed, AFM) may be entered.

The temperature of the smaller peak in $\partial(\chi'_H T)/\partial T$, which remains almost constant at $T=8$ K as the field is increased, is used to mark the additional H-T phase boundary (Fig. 11) into the 2D canted magnetic state.

Noting the magnetic transition at 8 K, the phenomena at 8 K and 9.5 kOe are of interest. Hysteresis in the isothermal dc curves is observed below 8 K and 9.5 kOe (see Fig. 6). In a constant field of 9.5 kOe, the main peak and smaller shoulder in $\chi'_H(T)$ merge at a temperature of 8 K (see Fig. 1). While the main peak in $\chi''_H(T)$ remains at a constant temperature (7.5 K) for $H \leqslant 9.5$ kOe, the peak temperature decreases for $H \geqslant 9.5$ kOe (see Fig. 2). The magnitudes of $\chi'_H(T)$ and $\chi''_H(T)$ are maximized at 9.5 kOe. The overall maximum value of $\chi'_T(H)$ occurs at 9.5 kOe at $T \sim 8$ K (see Fig. 3). In general, at 8 K and 9.5 kOe, the susceptibility is maximized. Examination of the proposed phase diagram of Fig. 11 suggests that 9.5 kOe and 8 K may mark a multicritical point, from which a variety of magnetic phases may be entered. This maximization of χ may be related to the coexistence of multiple phases.

The abrupt increases in the isothermal dc magnetization data below 4.2 K (Fig. 5) indicate metamagnetism. In a metamagnet, interchain couplings are broken under the application of a sufficiently strong field. Below 4.2 K in our

compound, the field of maximum dM/dH is observed to increase rapidly with decreasing temperature (Fig. 11), unlike the behavior above 4.2 K where it remains relatively constant (see Fig. 5 of Ref. 7). Below 2.2 K, the two steps observed in $M(H)$ indicate an additional higher-field transition, also displayed in the phase diagram of Fig. 11.

The nature of the phase intermediate to the AFM and paramagnetic states implied by the two transitions occurring below 2.2 K is of interest. Two different physical explanations are considered: the existence of multiple (greater than two) magnetic sublattices[21] and the existence of multiple metastable canting angles.[22] The occurrence of similar steplike behavior in $M(H)$ has been observed in the linear chain magnets[23] $FeCl_2 \cdot 2H_2O$, $CoCl_2 \cdot 2H_2O$, and $CoBr_2 \cdot 2H_2O$ in which, similar to the [MnOEP][HCBD], the intrachain interactions are significantly stronger than the interchain interactions. Both four and six magnetic sublattices have been proposed for these systems, in which only some subset of the chains are rotated by a single field, as opposed to a simple two sublattice system in which all the chains of antiparallel spins are rotated by a single field. The six sublattice model predicts the 3:1 ratio of the saturation magnetization to that of the intermediate state observed in the above family. For this reason, in addition to neutron data, the six-sublattice description is favored when describing this family.[12] In contrast, the ratio of the saturation magnetization to that of the intermediate state in the [MnOEP][HCBD] of $\sim 17/7 = 2.4$ (Fig. 5) is inconsistent with either a four or six multiple sublattice picture, which predict either 3:1, 3:2 or 2:1 ratios. In addition, the low-temperature magnetization data fits well with the predictions of a two-sublattice model (Fig. 9). For these reasons, a multiple-metastable canting angle description, in which metastable configurations corresponding to different cant angles are achieved enroute to saturation, is more likely than the multiple-sublattice description.

At 1.7 K, the behavior of $M(H)$ changes relative to the behavior between 1.8 and 2.2 K. Two transitions are observed, however, the lower-field transition (occurring at 19 kOe) is extremely abrupt while the higher field transition (occurring at 25 kOe) is less abrupt and therefore more closely resembles a spin-flop transition. In addition, the magnetization of the intermediate state is $\sim 10\,000$ emuG/mol as opposed to the ~ 7000 emuG/mol observed between 1.8 and 2.2 K. This change in behavior at 1.7 K suggests yet another magnetic transition.

C. Interchain coupling and dipole-dipole interactions

The weak ferromagnetic states occurring below 4.2 and 8 K require net interchain interactions that are both antisymmetric[18] and anisotropic. We discuss the interchain exchange, single-ion anisotropy and interchain dipole-dipole interactions and their relative importance in creating these states. A cross-sectional view of the [MnOEP][HCBD] chain compound[1,5] reveals four neighbor chains with two at a distance of 8.02 Å and two at 12.33 Å. The interchain exchange in most members of the metalloporphyrin family, has been estimated to be negligible due to large interchain distances, the bulkiness of the porphyrins, and the lack of conjugation between the porphyrin and its substituent groups.[8] The [MnOEP][HCBD] represents an exception in that its exchange has been estimated to be non-negligible[8] (~ 0.1 K) along one interchain axis and is presumed responsible for the 2D AFM ordering process occurring at 19.6 K. The exchange along the other interchain axis is expected to be significantly weaker. On the other hand, previous studies[8] have determined that the interchain dipole-dipole interactions have sufficient energy to influence the magnetic state of this and other members of the metalloporphyrin family near 10 K and below.

A system of chains coupled via dipole-dipole interactions will be anisotropic as a result of the anisotropy of this interaction. The competition between single-ion anisotropy, with its own preferred orientation of the spins, and the anisotropic dipole-dipole interactions of the chains allows the possibility of canting.[5,8] The interchain dipole energy between two $S = 2$ units separated by the interchain distance of 8.02 Å is estimated at ~ 0.02 K using the point-dipole approximation. The single-ion anisotropy on the $S = 2$ site is estimated of the order 1 K, 50 times larger than the dipole-dipole energy, and thus the dominant factor determining a preferred spin orientation in this system.

According to the point-dipole approximation, the dipole-dipole energy decreases with distance as r^{-3}, thus a rough estimate of the relative strengths of the dipole-dipole interactions along the two interchain axes is given by $(12.33)^3/(8.02)^3 = 3.6$. This approximately 4 to 1 ratio suggests that the interactions along the closer interchain axis become relevant earlier than those along the farther axis. Thus the transition at 8 K is related to interchain dipole-dipole interactions along the nearer interchain axis, and the transition at 4.2 K results from the 3D coupling, via the dipole-dipole interactions along the farther interchain direction, of the sheets formed at 8 K.

V. CONCLUSION

Magnetization and susceptibility studies of [MnOEP][HCBD] reveal transitions at 8 K and 4.2 K (in zero field) in addition to the earlier reported 19.6 K transition. The transition at 8 K, is marked by a shoulder in χ', the appearance of nonzero χ'', and dc hysteresis with no coercive field or spontaneous moment. The transition at 4.2 K is marked by dc irreversibilities, the appearance of a spontaneous moment and nonzero coercive fields. The disappearance of the spontaneous moment is well fit by a power law in reduced temperature with the critical exponent $\beta = 0.31$ indicating a 3D Ising-like transition. The behavior of the spontaneous moment sufficiently below T_c fits the two-sublattice canted antiferromagnetic description well.

The phase boundaries have been mapped using both ac and dc techniques. The resulting phase diagram shows the ac and dc boundary determinations to be self-consistent. A tricritical point has been identified at 2 kOe and 19.6 K. A multicritical point has been identified at 9.5 kOe and 8 K. Below 2.2 K multiple magnetic transitions are evident. The data suggest that the transitions at 8 and 4.2 K are to two and three dimensionally coupled weak ferromagnetic states, respectively. Interchain dipole-dipole interactions are proposed as the cause of the transitions.

In summary, we propose the following description of the evolution of the magnetic state of [MnOEP][HCBD]. At high temperatures (room temperature) the system behaves as Heisenberg-like ferrimagnetic chains. At 19.6 K, the system is coupled into sheets of Ising-like antiferromagnetically coupled chains due to single-ion anisotropy and interchain exchange. At 8 K, the dipole interactions between chains within these sheets creates a system of 2D canted chains. At 4.2 K, these sheets are coupled into a 3D canted system via dipole interactions along the farther interchain direction.

ACKNOWLEDGMENTS

This work was supported in part by the DOE under Grants No. DE-FG02-86BR45271 and DE-FG03-93ER45504, and by the NSF under Grant No. CHE9320478. We thank K-I. Sugiura and X. Wang for preparing some samples.

[1] J. S. Miller, C. Vazquez, N. L. Jones, R. S. McLean, and A. J. Epstein, J. Mater. Chem. **5**, 707 (1995).

[2] J. S. Miller, J. Calabrese, R. S. McLean, and A. J. Epstein, Adv. Mater. **4**, 498 (1992).

[3] A. Bohm, C. Vazquez, R. S. McLean, J. C. Calabrese, S. Kalm, J. Manson, A. J. Epstein, and J. S. Miller, Inorg. Chem. **35**, 3083 (1996).

[4] K-I. Sugiura, A. Arif, D. K. Rittenberg, J. Schweizer, L. Ohrstrom, A. J. Epstein, and J. S. Miller, Chem. Eur. J. **3**, 138 (1997).

[5] C. M. Wynn, M. A. Gîrţu, K-I. Sugiura, E. J. Brandon, J. L. Manson, J. S. Miller, and A. J. Epstein, Synth. Met. **85**, 1695 (1997).

[6] A. J. Epstein, C. M. Wynn, M. A. Gîrţu, W. B. Brinckerhoff, E. J. Brandon, K-I. Sugiura, and J. S. Miller, Mol. Cryst. Liq. Cryst. Sci. Technol., Sect. A **305**, 321 (1997).

[7] C. M. Wynn, M. A. Gîrţu, J. S. Miller, and A. J. Epstein, Phys. Rev. B **56**, 315 (1997).

[8] C. M. Wynn, M. A. Gîrţu, W. B. Brinckerhoff, K-I. Sugiura, J. S. Miller, and A. J. Epstein, Chem. Mater. **9**, 2156 (1997).

[9] L. N. Mulay, *Magnetic Susceptibility* (Wiley, New York, 1963).

[10] M. E. Fisher, Philos. Mag. **7**, 1731 (1962).

[11] F. Palacio, F. J. Lazaro, and A. J. Van Duyneveldt, Mol. Cryst. Liq. Cryst. **176**, 289 (1989).

[12] E. Stryjewski and N. Giordano, Adv. Phys. **26**, 487 (1977).

[13] A. Rouco, X. Obradors, M. Tovar, F. Perez, D. Chateigner, and P. Bordet, Phys. Rev. B **50**, 9924 (1994).

[14] J. J. Binney, N. J. Dowrick, A. J. Fisher, and M. E. J. Newman, *The Theory of Critical Phenomena* (Oxford University, New York, 1995), p. 20.

[15] L. J. de Jongh, *Magnetic Properties of Layered Transition Metal Compounds* (Kluwer, Boston, 1990).

[16] M. A. Gîrţu, C. M. Wynn, K-I. Sugiura, J. S. Miller, and A. J. Epstein, Synth. Met. **85**, 1703 (1997).

[17] O. Kahn, *Molecular Magnetism* (VCH, New York, 1993), p. 140.

[18] T. Moriya, in *Magnetism*, edited by G. Rado and H. Suhl (Academic, New York, 1963), Vol. I, p. 115.

[19] J. M. Kincaid and E. G. D. Cohen, Phys. Rep., Phys. Lett. **22C**, 57 (1975).

[20] R. Hoogerbeets, S. A. J. Wiegers, A. J. Van Duyneveldt, R. D. Willett, and U. Geiser, Physica B & C **125**, 135 (1984).

[21] T. Oguchi, J. Phys. Soc. Jpn. **20**, 2236 (1965); A. Narath, Phys. Lett. **13**, 12 (1964); K. Yamada and J. Kanamori, Prog. Theor. Phys. **38**, 541 (1967).

[22] H. Kobayashi and T. Haseda, J. Phys. Soc. Jpn. **19**, 765 (1964).

[23] A. Narath, Phys. Rev. **139**, A1221 (1965); J. Phys. Soc. Jpn. **19**, 2244 (1964).